Available online at www.sciencedirect.com
ScienceDirect
Transportation Research Part C 16 (2008) 731–741
TRANSPORTATION RESEARCH PART C
www.elsevier.com/locate/trc

Designing a sliding mode controller for slip control of antilock brake systems

A. Harifi, A. Aghagolzadeh *, G. Alizadeh, M. Sadeghi

Faculty of Electrical and Computer Engineering, University of Tabriz, Tabriz 51664, Iran

Received 18 January 2007; received in revised form 14 February 2008; accepted 25 February 2008

Abstract

Antilock brake system (ABS) has been designed to achieve maximum negative acceleration by preventing the wheels from locking. Research shows that the friction between road and tire is a nonlinear function of wheel slip. Therefore, maximum negative acceleration can be achieved by designing a suitable control system for wheel slip regulation at its optimum value. Since there is a lot of nonlinearity and uncertainty (uncertainty in mass and center of gravity of the vehicle and road condition) in vehicle dynamics, a robust control method should be used. In this research, a sliding mode controller for wheel slip control has been designed based on a two-axle vehicle model. Important considered parameters for vehicle dynamic include two separated brake torques for front and rear wheels as well as longitudinal weight transfer caused by the acceleration or deceleration. One of the common problems in sliding mode control is chattering phenomenon. In this paper, primary controller design has been improved using integral switching surface to reduce chattering effects. Simulation results show the success of integral switching surface in elimination of chattering side effects and by high performance of this controller. At the end, the performance of the designed controller has been compared with three of the prevalent papers results to determine the performance of sliding mode control integrated with integral switching surface.

Keywords: Antilock brake system; Integral switching surface; Sliding mode control

1. Introduction

Antilock Brake System is one of the most important systems which is used in vehicles nowadays to improve the safety of the driver and passengers. The main idea of ABS is to attain the optimum negative acceleration rate without sacrificing the stability and steering ability of the vehicle (Kueon and Bedi, 1995).

When a vehicle is braking or accelerating, the tractive forces produced by the tire are proportional to the normal forces of the road acting on the tire. The coefficient of this proportion, denoted μ, is called road coefficient of adhesion (or friction coefficient) and varies depending on the road surface. Researches show that the road coefficient of adhesion is a nonlinear function of wheel slip (λ) in a specified road condition (Fig. 1).

* Corresponding author. Tel.: +98 411 339 3720; fax: +98 411 3300819.
E-mail addresses: a_harifi@tabrizu.ac.ir (A. Harifi), aghagol@tabrizu.ac.ir (A. Aghagolzadeh).

0968-090X/$ - see front matter © 2008 Elsevier Ltd. All rights reserved.
doi:10.1016/j.trc.2008.02.003

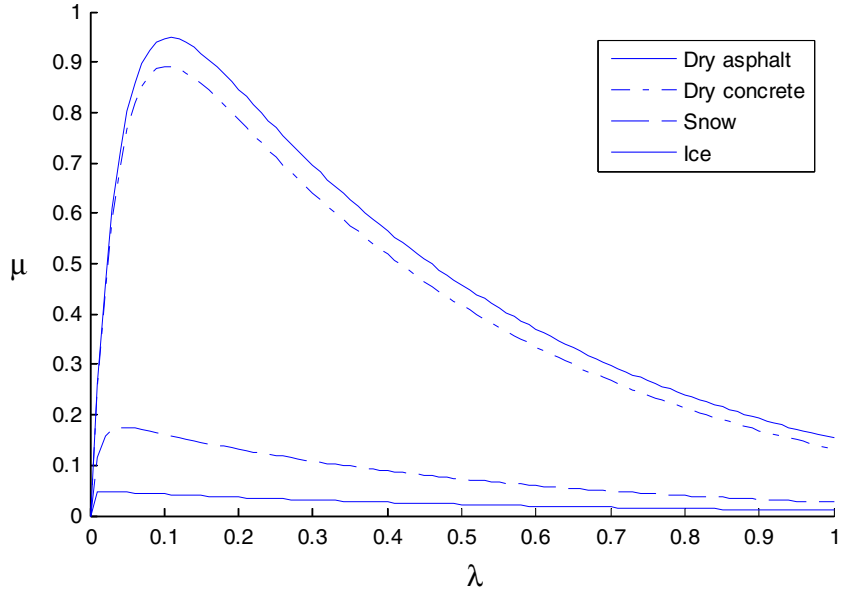

Fig. 1. A typical μ–λ curve.

Therefore the most important goal in designing a controller for ABS is to design a suitable controller which can regulate the real wheel slip at its optimum value.

Antilock brake systems present a challenging control problem because (Akbarzadeh et al., 2002):

1. vehicle model dynamics are highly nonlinear;
2. controller must operate at unstable equilibrium point for optimal performance;
3. model parameters vary over a wide range due to variations of road and vehicle conditions such as road surface, mass and center of gravity of the vehicle;
4. sensor signals are highly uncertain as noisy.

Therefore, it seems that a robust controller should be used for solving these control problems. The sliding mode control is a common robust control method. Hence a lot of researches are based on the sliding mode control method (Chin et al., 1992; Drakunov et al., 1995; Lin and Hsu, 2003a, 2003b; Ming, 1997; Tan and Tomizuka, 1989; Unsal and Kachroo, 1999).

Lin and Hsu used a neural network estimator to estimate the uncertainty of the system to reduce chattering phenomena which is produced by sliding mode control (Lin and Hsu, 2003a).

In another paper, Lin and Hsu introduced a fuzzy controller combined with sliding mode control to reduce the dependency of controller on vehicle model (Lin and Hsu, 2003b).

Unsal and Kachroo have used sliding mode control to regulate wheel slip at its optimum value too. In their paper, a PI-like controller was used near the switching surface instead of sign function to reduce chattering (Unsal and Kachroo, 1999).

In this paper, the control strategy is sliding mode control too. But unlike other papers, the controller has been designed based on a two-axle vehicle model. Important considered parameters for vehicle dynamic include two separated brake torques for front and rear wheels as well as longitudinal weight transfer caused by the acceleration or deceleration. Then the primary controller design has been improved using integral switching surface to reduce chattering phenomena. At the end, the desired controller has been compared with the controllers introduced in Lee and Zak (2002) and Lin and Hsu (2003a,b). Simulation results show the success of integral switching surface in significant reduction of chattering and high performance of this controller with respect other controllers.

2. Vehicle dynamic and tire friction models

The first step in the controller design procedure is finding a truth model of the dynamics of the process to be controlled. In this paper, the vehicle model given in Lee and Zak (2002) has been used. Fig. 2 shows the vehicle free body diagram.

Assuming x, v, ω_f, ω_r, T_{bf} and T_{br} as vehicle position, vehicle speed, angular velocity of front and rear wheel, front and rear brake torque, respectively, we have:

$$\begin{cases} \dot{x} = v \\ \dot{v} = -g\frac{\mu(\lambda_f)m_1+\mu(\lambda_r)m_2}{m_{tot}-\mu(\lambda_f)m_3+\mu(\lambda_r)m_3} \\ \dot{\omega}_f = \frac{1}{2J_f}(-T_{bf}+\mu(\lambda_f)m_1R_\omega g-\mu(\lambda_f)m_3R_\omega\ddot{x}) \\ \dot{\omega}_r = \frac{1}{2J_r}(-T_{br}+\mu(\lambda_r)m_2R_\omega g+\mu(\lambda_f)m_3R_\omega\ddot{x}) \end{cases} \tag{1}$$

where

$$m_1 = \frac{b}{a+b}m_{tot}$$

$$m_2 = \frac{a}{a+b}m_{tot}$$

$$m_3 = \frac{m_f h_f + m_s h_s + m_r h_r}{a+b}$$

Table 1, defines all constants and their nominal values which used in Eq. (1). Since the main goal is wheel slip control, the state space equation should be rewritten based on front and rear wheel slips. The front and rear wheel slips and their derivatives are defined as

$$\lambda_f = \frac{v-\omega_f R_\omega}{v} \Rightarrow \dot{\lambda}_f = \frac{\dot{v}(1-\lambda_f)-\dot{\omega}_f R_\omega}{v} \tag{2}$$

$$\lambda_r = \frac{v-\omega_r R_\omega}{v} \Rightarrow \dot{\lambda}_r = \frac{\dot{v}(1-\lambda_r)-\dot{\omega}_r R_\omega}{v} \tag{3}$$

Substituting (2) and (3) into (1), we obtain

$$\begin{cases} \dot{x} = v \\ \dot{v} = f_2(\lambda_f,\lambda_r) \\ \dot{\lambda}_f = \frac{f_2(\lambda_f,\lambda_r)(1-\lambda_f)-R_\omega f_3(\lambda_f,\lambda_r)+u_f}{v} \\ \dot{\lambda}_r = \frac{f_2(\lambda_f,\lambda_r)(1-\lambda_r)-R_\omega f_4(\lambda_f,\lambda_r)+u_r}{v} \end{cases} \tag{4}$$

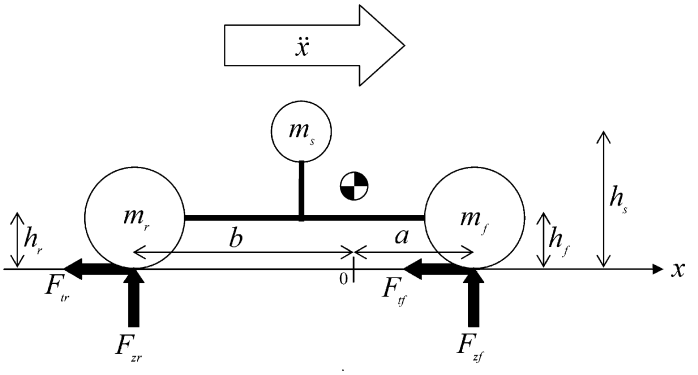

Fig. 2. The vehicle free body diagram (Lee and Zak, 2002).

Table 1
Vehicle model data (Lee and Zak, 2002)

Symbol	Quantity	Value
g	Acceleration due to gravity	9.81 m/s^2
a	Distance from center of gravity to front axle	1.186 m
b	Distance from center of gravity to rear axle	1.258 m
h_s	Height of the sprung mass	0.6 m
h_f	Height of front unsprung mass	0.3 m
h_r	Height of rear unsprung mass	0.3 m
m_{tot}	Total mass of the vehicle	1500 kg
m_s	Sprung mass of the vehicle	1285 kg
m_f	Front unsprung mass	96 kg
m_r	Rear unsprung mass	119 kg
J_f	Moment of inertia of the front wheel	1.7 kg m^2
J_r	Moment of inertia of the rear wheel	1.7 kg m^2
R_ω	Radius of tire	0.326 m

where

$$f_2(\lambda_f, \lambda_r) = -g\frac{\mu(\lambda_f)m_1 + \mu(\lambda_r)m_2}{m_{tot} - \mu(\lambda_f)m_3 + \mu(\lambda_r)m_3} \tag{5}$$

$$f_3(\lambda_f, \lambda_r) = \frac{1}{2J_f}(\mu(\lambda_f)m_1R_\omega g - \mu(\lambda_f)m_3R_\omega f_2) \tag{6}$$

$$f_4(\lambda_f, \lambda_r) = \frac{1}{2J_r}(\mu(\lambda_r)m_2R_\omega g + \mu(\lambda_f)m_3R_\omega f_2) \tag{7}$$

$$u_f = \frac{R_\omega T_{bf}}{2J_f} \tag{8}$$

$$u_r = \frac{R_\omega T_{br}}{2J_r} \tag{9}$$

In this paper, the tire friction model introduced by Burckhardt (1993) has been used to simulate antilock brake system. It provides the tire-road coefficient of friction μ as a function of the wheel slip λ and the vehicle velocity v.

$$\mu_x(\lambda, v) = (C_1(1 - e^{-C_2\lambda}) - C_3\lambda)e^{-C_4\lambda v} \tag{10}$$

The parameters in (10) denote the following: C_1 is the maximum value of friction curve; C_2 the friction curve shape; C_3 the friction curve difference between the maximum value and the value at $\lambda = 1$; and C_4 is the wetness characteristic value and is in the range 0.02–0.04 s/m.

Table 2 shows friction model parameters for different road conditions.

3. Sliding mode controller design

3.1. Bounds of uncertainties

One of the most important steps in controller design procedure is to find the proper bounds of uncertainty. For this purpose, it has been assumed that uncertainty of nonlinear functions have risen out of uncertainty of m_1, m_2, m_3, m_{tot} and μ variables.

Table 2
Friction model parameters (Burckhardt, 1993)

Surface conditions	c_1	c_2	c_3
Dry asphalt	1.2801	23.99	0.52
Wet asphalt	0.857	33.822	0.347
Dry concrete	1.1973	25.168	0.5373
Snow	0.1946	94.129	0.0646
Ice	0.05	306.39	0

$$m_1^- \leqslant m_1 \leqslant m_1^+$$
$$m_2^- \leqslant m_2 \leqslant m_2^+$$
$$m_3^- \leqslant m_3 \leqslant m_3^+$$
$$m_{\text{tot}}^- \leqslant m_{\text{tot}} \leqslant m_{\text{tot}}^+$$
$$0 \leqslant \mu(\lambda_f), \mu(\lambda_r) \leqslant 1$$

Based on Eq. (5), it can be easily seen that f_2 takes its minimum and maximum values when we have $\mu(\lambda_f) = \mu(\lambda_r) = 1$ and $\mu(\lambda_f) = \mu(\lambda_r) = 0$, respectively.

$$-g \leqslant f_2(\lambda_f, \lambda_r) \leqslant 0 \;\Rightarrow\; \hat{f}_2(\lambda_f, \lambda_r) = -0.5g \tag{11}$$

Considering (11), Eq. (6) shows that f_3 is always non negative. So f_3 takes its minimum value when $\mu(\lambda_f) = 0$. In the same way, we can see that assuming $f_2 = -g$, f_3 takes its maximum value if $\mu(\lambda_f)$, $\mu(\lambda_r)$, m_1 and m_3 take their maximum values.

$$0 \leqslant f_3 \leqslant \frac{R_\omega g}{2J_f}(m_1^+ + m_3^+) \;\Rightarrow\; \hat{f}_3 = \frac{R_\omega g}{4J_f}(m_1^+ + m_3^+) \tag{12}$$

The second term of Eq. (7) is always non positive. So finding the minimum and maximum values of f_4 is more complicated than f_3. If $m_2^- < m_3^+$ then f_4 may takes a negative value. Otherwise the minimum value of f_4 will be zero. On the other hand, f_4 takes its maximum value for $\mu(\lambda_f) = 0$, $\mu(\lambda_r) = 1$ and $m_2 = m_2^+$.

$$\min\left[\frac{R_\omega g}{2J_r}(m_2^- - m_3^+), 0\right] \leqslant f_4 \leqslant \frac{R_\omega g}{2J_r} m_2^+ \Rightarrow \hat{f}_4 = \frac{1}{2}\left(\min\left[\frac{R_\omega g}{2J_r}(m_2^- - m_3^+), 0\right] + \frac{R_\omega g}{2J_r} m_2^+\right) \tag{13}$$

assuming $|f_2 - \hat{f}_2| \leqslant F_2, |f_3 - \hat{f}_3| \leqslant F_3$ and $|f_4 - \hat{f}_4| \leqslant F_4$ implies

$$F_2 = 0.5g \tag{14}$$
$$F_3 = \frac{R_\omega g}{4J_f}(m_1^+ + m_3^+) \tag{15}$$
$$F_4 = \frac{R_\omega g}{2J_r} m_2^+ - \frac{1}{2}\left(\min[\frac{R_\omega g}{2J_r}(m_2^- - m_3^+), 0] + \frac{R_\omega g}{2J_r} m_2^+\right) \tag{16}$$

3.2. Controller design

Consider the nonlinear vehicle model with uncertainties (17)

$$\begin{cases} \dot{x} = v \\ \dot{v} = f_2(\lambda_f, \lambda_r) \\ \dot{\lambda}_f = \frac{f_f(\lambda_f, \lambda_r) + u_f}{v} |f_f(\lambda_f, \lambda_r) - \hat{f}_f(\lambda_f, \lambda_r)| \leqslant F_f(\lambda_f, \lambda_r) \\ \dot{\lambda}_r = \frac{f_r(\lambda_f, \lambda_r) + u_r}{v} |f_r(\lambda_f, \lambda_r) - \hat{f}_r(\lambda_f, \lambda_r)| \leqslant F_r(\lambda_f, \lambda_r) \end{cases} \tag{17}$$

where:

$$f_f(\lambda_f, \lambda_r) = f_2(\lambda_f, \lambda_r)(1 - \lambda_f) + R_\omega f_3(\lambda_f, \lambda_r) \tag{18}$$
$$\hat{f}_f(\lambda_f, \lambda_r) = \hat{f}_2(\lambda_f, \lambda_r)(1 - \lambda_f) + R_\omega \hat{f}_3(\lambda_f, \lambda_r) \tag{19}$$
$$F_f(\lambda_f, \lambda_r) = F_2(1 - \lambda_f) + R_\omega F_3 \tag{20}$$
$$f_r(\lambda_f, \lambda_r) = f_2(\lambda_f, \lambda_r)(1 - \lambda_r) + R_\omega f_4(\lambda_f, \lambda_r) \tag{21}$$
$$\hat{f}_r(\lambda_f, \lambda_r) = \hat{f}_2(\lambda_f, \lambda_r)(1 - \lambda_r) + R_\omega \hat{f}_4(\lambda_f, \lambda_r) \tag{22}$$
$$F_r(\lambda_f, \lambda_r) = F_2(1 - \lambda_r) + R_\omega F_4 \tag{23}$$

The control objective is to find control inputs u_f and u_r in someway that state variable λ_f and λ_r track the desired trajectory λ_{fd} and λ_{rd}, respectively. Defining switching surface as

$$s_1 = \tilde{\lambda}_f = \lambda_f - \lambda_{fd} \tag{24}$$

$$s_2 = \tilde{\lambda}_r = \lambda_r - \lambda_{rd} \tag{25}$$

implies

$$\begin{aligned} &u_{eqf} = \dot{\lambda}_{fd} v - \hat{f}_f(\lambda_f, \lambda_r) \\ &\Rightarrow u_f = \dot{\lambda}_{fd} v - \hat{f}_f(\lambda_f, \lambda_r) - (F_f(\lambda_f, \lambda_r) + \eta_1 \mathrm{sign}(\tilde{\lambda}_f)) \end{aligned} \tag{26}$$

$$\begin{aligned} &u_{eqr} = \dot{\lambda} v - \hat{f}_f(\lambda_f, \lambda_r) \\ &\Rightarrow u_r \dot{\lambda}_{rd} v - \hat{f}_f(\lambda_f, \lambda_r) - (F_f(\lambda_f, \lambda_r) + \eta_2 \mathrm{sign}(\tilde{\lambda}_f)) \end{aligned} \tag{27}$$

where η_1 and η_2 are positive constants.

3.3. Chattering reduction

Chattering phenomena is one of the undesirable effects of sliding mode control. The main reason of chattering phenomena is the existence of sign function in control inputs u_f and u_r. Different methods for chattering reduction are introduced (Kachroo and Tomizuka, 1996; Slotine and Li, 1991; Slotine and Sastry, 1983). In this paper, integral switching surface is suggested for solving this problem. Defining integral switching surface as

$$s_1 = \tilde{\lambda}_f + \alpha_1 \int \tilde{\lambda}_f \, dt = \lambda_f - \lambda_{fd} + \alpha_1 \int \tilde{\lambda}_f \, dt \tag{28}$$

$$s_2 = \tilde{\lambda}_r + \alpha_2 \int \tilde{\lambda}_r \, dt = \lambda_r - \lambda_{rd} + \alpha_2 \int \tilde{\lambda}_r \, dt \tag{29}$$

the following relations are obtained:

$$\begin{aligned} u_{eqf} &= (\dot{\lambda}_{fd} - \alpha_1 \tilde{\lambda}_f) v - \hat{f}_f(\lambda_f, \lambda_r) \\ u_{eqr} &= (\dot{\lambda}_{rd} - \alpha_2 \tilde{\lambda}_r) v - \hat{f}_r(\lambda_f, \lambda_r) \end{aligned} \tag{30}$$

$$\Rightarrow u_r = (\dot{\lambda}_{rd} - \alpha_2 \tilde{\lambda}_r) v - \hat{f}_r - (F_r + \eta_2) \mathrm{sat}\left(\frac{\tilde{\lambda}_r + \alpha_2 \int \tilde{\lambda}_r \, dt}{\varphi_2} \right) \tag{31}$$

4. Simulation results

To simulate the designed ABS it has been assumed that the uncertainties of functions have risen out of 20% uncertainty in center of gravity and 30% uncertainty in total mass of the vehicle. From Fig. 1, it can be seen that the maximum friction is achieved near $\lambda = 0.15$. Thus, the step response of the first order system $0.15 \times \frac{20}{s+20}$ was assumed as desired slip of the front and rear wheels. Further, it was assumed that the velocity of vehicle was 20 m/s (equivalently 72 km/h) before braking and the vehicle moves along a straight path.

It can be seen in Fig. 3 that differential switching surface causes chattering in front and rear brake torques. Figs. 4 and 5 show that sliding mode controller with integral switching surface is a suitable and successful method to control wheel slip without chattering.

Fig. 6 shows the performance of sliding mode controller with integral switching surface for variable road condition. In this simulation it has been assumed that after 5 m, the road condition changes from dry asphalt to wet asphalt and after 15 m, it changes from wet asphalt to snow. Again, results confirm the ability of controller in wheel slip control.

Since the vehicle model of this paper is similar to vehicle model of Lee and Zak (2002), simulation result of Lee and Zak (2002) has been presented in Fig. 7. The results show that the Genetic Algorithm adjusted Fuzzy Controller causes chattering and does not seem suitable to control wheel slip, since the stability of vehicle system with fuzzy controller is unclear under uncertainty conditions. Proposed sliding mode controller outperforms the fuzzy controller in terms of the following reasons:

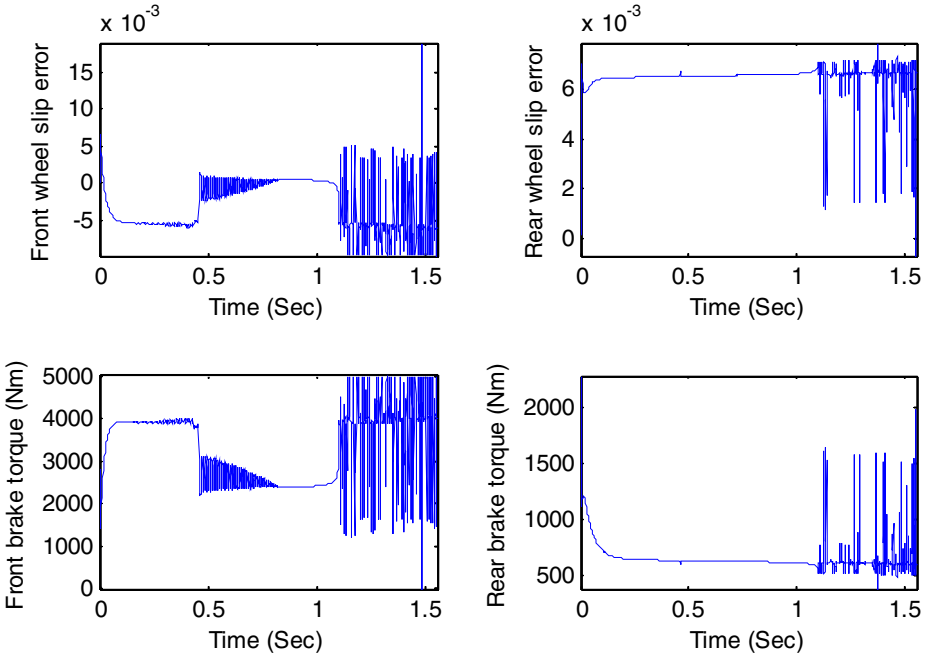

Fig. 3. Simulation results for differential switching surface with saturation function and dry asphalt.

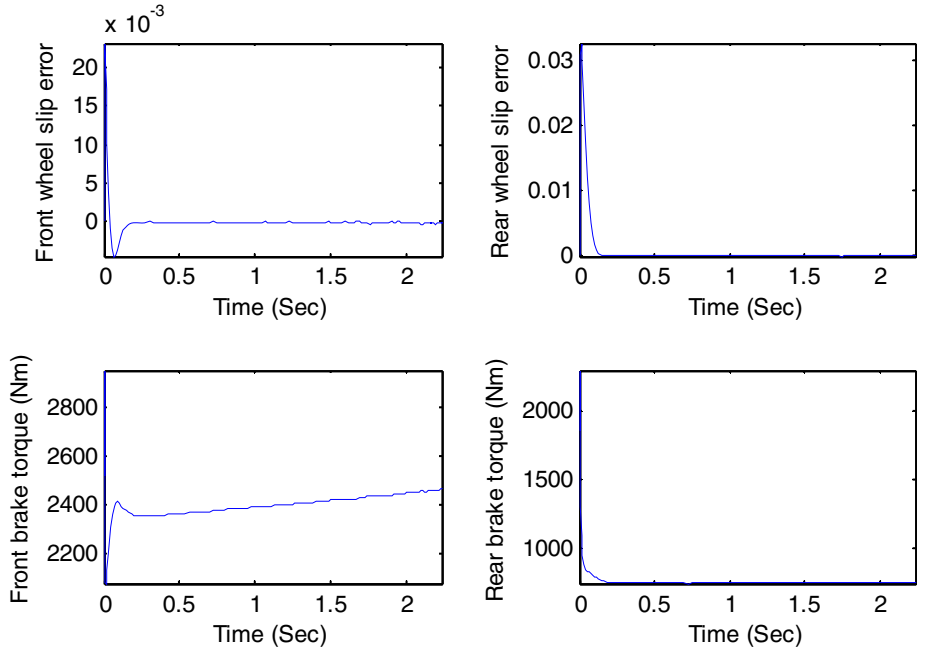

Fig. 4. Simulation results for integral switching surface with saturation function and dry asphalt.

Not only the simulation results but also the stability of the sliding mode controller is proven to be more robust and reliable than that of the fuzzy one. As the fuzzy controller was adjusted to the nominal status of the vehicle, it would lead to inappropriate reaction due to possible uncertainty in the automobile model.

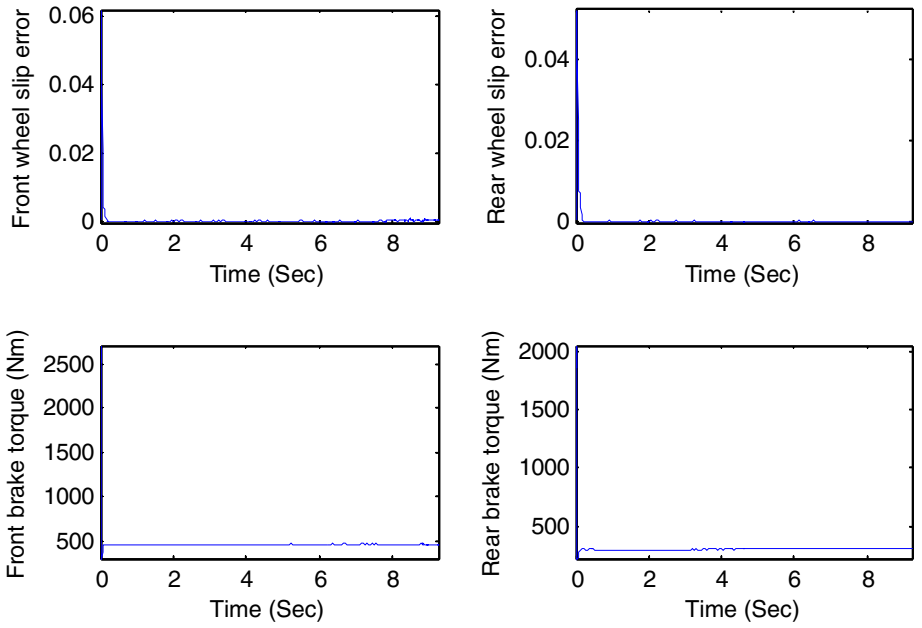

Fig. 5. Simulation results for integral switching surface with saturation function and snow.

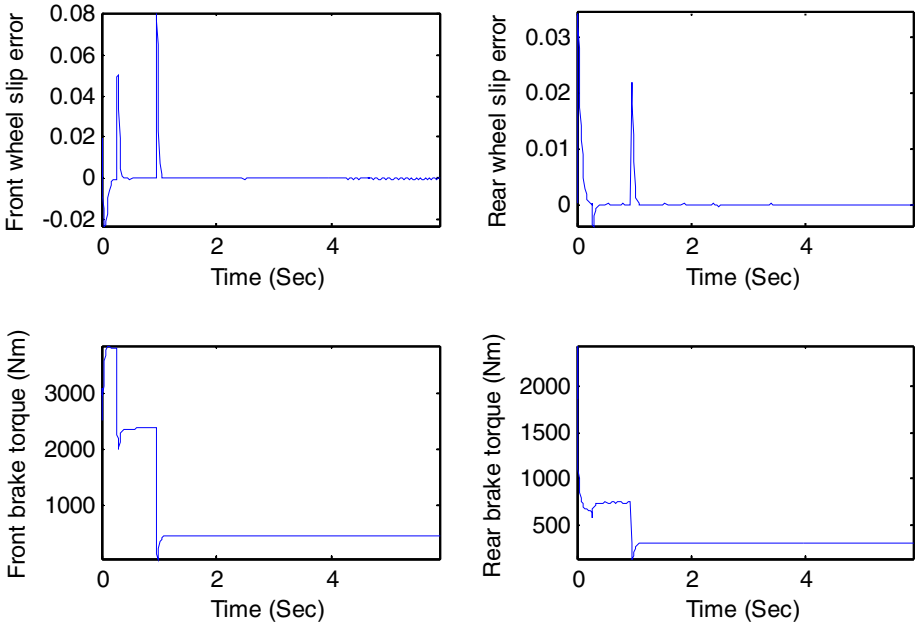

Fig. 6. Simulation results for the integral switching surface with the saturation function and variable road condition.

Two of the methods encompassing the sliding mode controller and integral switching surface concepts are self-learning fuzzy (Lin and Hsu, 2003b) and neural network hybrid (Lin and Hsu, 2003a) controllers which are designed on the basis of the simplified vehicle model i.e. sliding control is based on one brake torque (Figs. 8 and 9) whereas causes the low efficiency of the controllers which makes the ultimate stopping distance of the automobile intolerable in comparison to that obtained by the presented system.

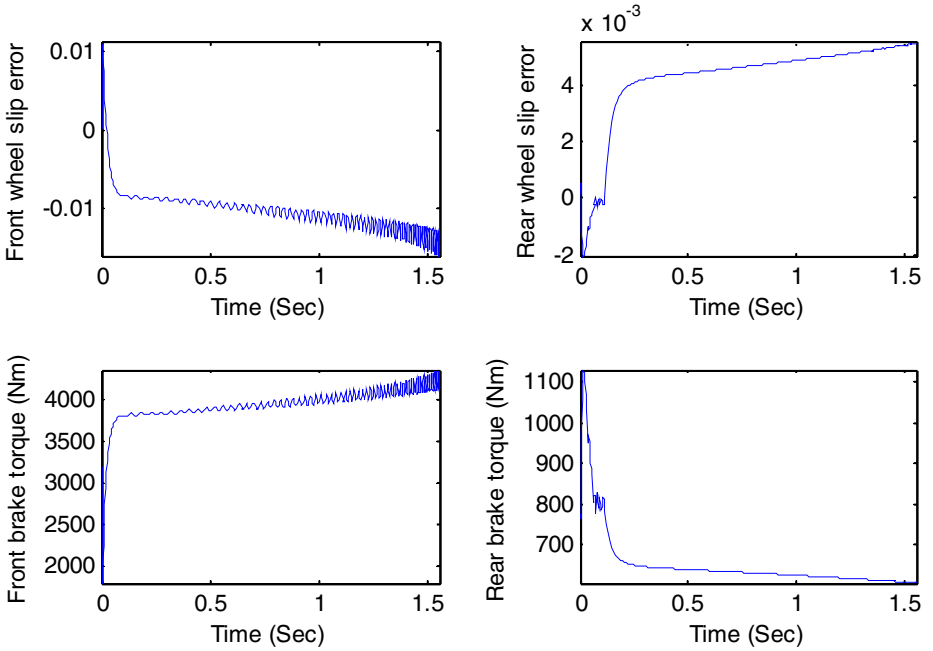

Fig. 7. Simulation results for genetic algorithm adjusted fuzzy controller and dry asphalt.

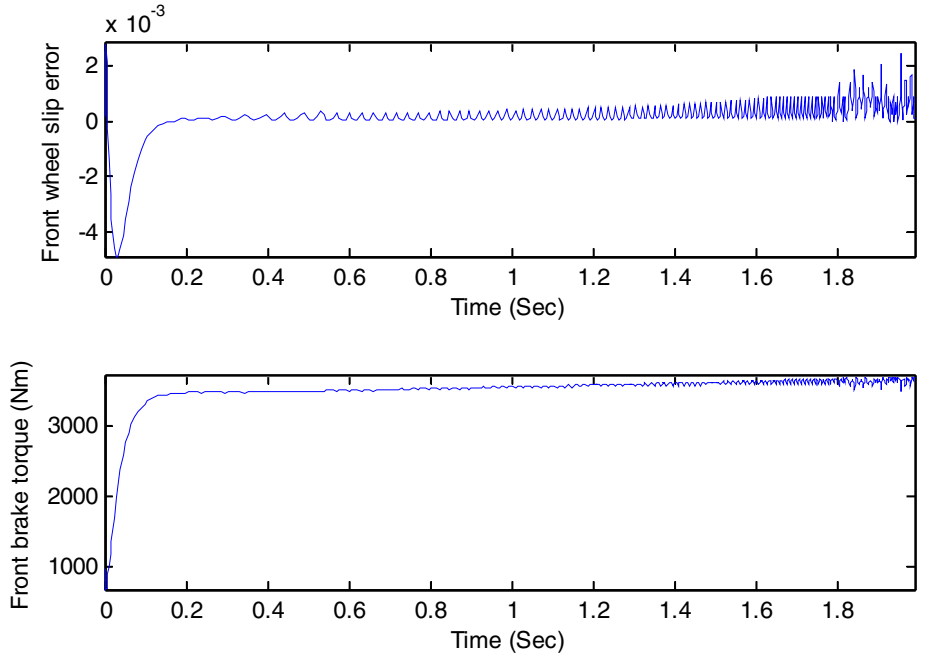

Fig. 8. Simulation results for self learning fuzzy-sliding mode controller and dry asphalt.

Table 3 shows the simulation results.

$J = \int_0^{t_f} (T_{bf}^2(t) + T_{br}^2(t))\,dt$ is used to compute the control energy, where T_{bf} and T_{br}, respectively, present the torque of the front and rear brake. Power spectral Density figures of brake torques are also used to determine the chattering rate of the torque values of both brakes. Percentage of slip error of front and rear wheels is determined by

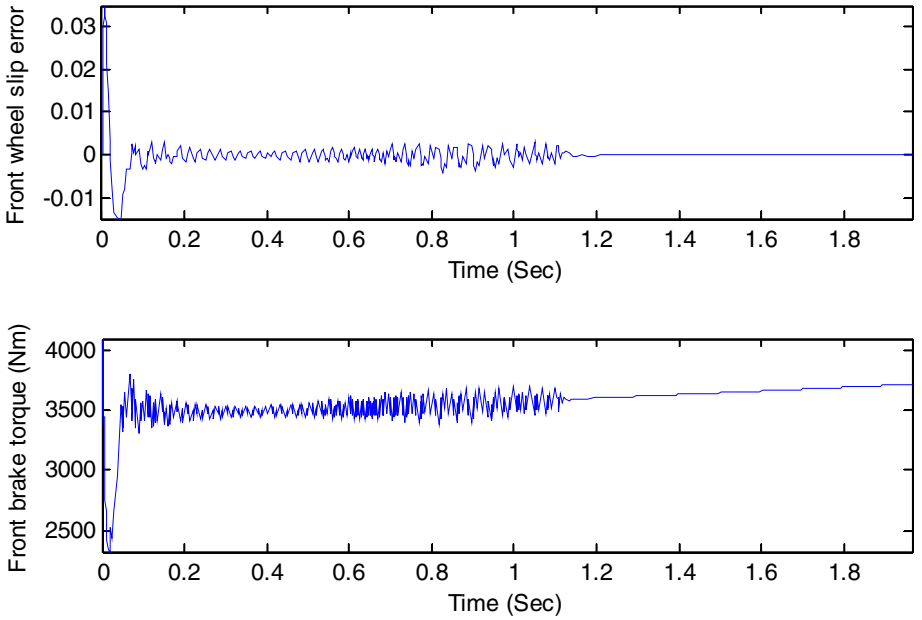

Fig. 9. Simulation results for neural network hybrid controller and dry asphalt.

Table 3
Simulation results

Controller	Road condition	Stop distance	Control energy ($\times 10^6$)	Chattering of front-brake torque	Chattering of rear-brake torque	Percentage of front wheel slip error	Percentage of rear wheel slip error
Proposed	Dry asphalt	18.05	23.96	57	41	0.46	0.48
Genetic adjusted fuzzy	Dry asphalt	18.8	24.12	153	46	6.89	2.91
Self learning fuzzy-sliding mode	Dry asphalt	23.41	24.91	112	–	0.08	–
Neural network hybrid	Dry asphalt	22.94	25.05	233	–	0.05	–
Proposed	Wet asphalt	25.87	14.06	38	33	0.02	0.59
Genetic adjusted fuzzy	Wet asphalt	25.93	13.85	424	41	6.09	1.08
Self learning fuzzy-sliding mode	Wet asphalt	37.95	15.12	108	–	0.21	–
Neural network hybrid	Wet asphalt	37.49	15.22	100	–	0.01	–
Proposed	Snow	106.5	2.807	31	26	0.74	0.65
Genetic adjusted fuzzy	Snow	107.2	2.853	399	6	37.94	28.32
Self learning fuzzy-sliding mode	Snow	186.9	2.919	139	–	0.58	–
Neural network hybrid	Snow	186.6	3.038	94	–	0.21	–

$$\text{Percentage of slip error} = \frac{\text{average of slip error}}{\text{average of reference slip}}$$

The results that are shown in Table 3 verify the better performance of proposed controller versus the other controllers (GA adjusted fuzzy controller, self learning fuzzy-sliding mode Controller and neural network hybrid controller) for three road condition (dry asphalt, wet asphalt and snow).

5. Conclusion

The proposed method presents a sliding mode control method to regulate slips in the front and rear wheel under specified bounds of uncertainty which utilizes integral switching surface in chattering reduction that proves thriving. In addition, the efficiency of the method surpasses the advantages of the fuzzy controller,

the neural network hybrid and Self learning fuzzy-sliding mode (as intelligent controllers) in ABS problem in terms of response smoothness and performance.

References

Akbarzadeh, M.R., Emami, K.J., Pariz, N., 2002. Adaptive discrete-time fuzzy sliding mode control for anti-lock braking systems. In: Annual Meeting of the North American Fuzzy Information Processing Society (NAFIPS), pp. 554–559.

Burckhardt, M., 1993. Fahrwerktechnik: Radschlupf-Regelsysteme. Vogel-Verlag, Wurtzburg.

Chin, Y.K., et al., 1992. Sliding-mode ABS wheel slip control. In: Proceedings of the ACC, Chicago, 24–26 June, pp. 1–6.

Drakunov, S., Ozguner, U., Dix, P., Ashrafi, B., 1995. ABS control using optimum search via sliding modes. IEEE Transactions on Control System Technology 3 (1).

Kachroo, P., Tomizuka, M., 1996. Chattering reduction and error convergence in the sliding-mode control of a class of nonlinear systems. IEEE Transactions on Automatic Control 41 (7), July 1996.

Kueon, Y.S., Bedi, J.S., 1995. Fuzzy-neural-sliding mode controller and its applications to the vehicle anti-lock braking systems. In: International IEEE/IAS Conference on Industrial Automation and Control: Emerging Technologies 22–27 May, pp. 391–398.

Lee, Y., Zak, S.H., 2002. Designing a genetic neural fuzzy antilock-brake-system controller. IEEE Transactions on Evolutionary Computation 6 (2).

Lin, C.M., Hsu, C.F., 2003a. Neural-network hybrid control for antilock braking systems. IEEE Transactions on Neural Networks 14 (2).

Lin, C.M., Hsu, C.F., 2003b. Self-learning fuzzy sliding-mode control for antilock braking systems. IEEE Transactions on Control System Technology 11 (2).

Ming, Q., 1997. Sliding mode controller design for ABS system. Master of Science Thesis, Faculty of the Virginia Polytechnic Institute, Virginia.

Slotine, J.J.E., Li, W., 1991. Applied Nonlinear Control. Prentice Hall, pp. 276–308.

Slotine, J.J.E., Sastry, S.S., 1983. Tracking control of nonlinear systems using sliding surfaces with application to robot manipulator. International Journal of Control 39 (2).

Tan, H.S., Tomizuka, M., 1989. An adaptive sliding mode vehicle traction controller design. In: Proceedings of the American Control Conference, pp. 1053–1058.

Unsal, C., Kachroo, P., 1999. Sliding mode measurement feedback control for antilock braking systems. IEEE Transactions on Control System Technology 7 (2).